A 350-GHz SIS Antipodal Finline Mixer

Ghassan Yassin, Stafford Withington, *Member, IEEE*, Matthew Buffey, K. Jacobs, *Member, IEEE*, and S. Wulff

***Abstract*—In this paper, we describe the design and operation of a 350-GHz finline superconductor–insulator–superconductor mixer. The mixer is fed by a horn–reflector antenna, and the superconducting circuit is fabricated using planar-circuit technology and fully integrated tuning. An important feature of the mixer is that it employs an antipodal finline section, deposited on one side of a quartz substrate, which transforms the high impedance of the waveguide (≈300 Ω) to the low impedance of the microstrip (≈20 Ω). The Nb/Al–oxide/Nb tunnel junction is fabricated at the same time as the finline circuit. In this paper, we describe the design procedure in some detail. We pay particular attention to the synthesis of the finline taper and the electromagnetic design of the horn–reflector antenna. We have tested a finline mixer over the frequency range of 330–370 GHz and measured a receiver noise temperature of 90 K, which remained unchanged over the whole frequency range. Our investigation has demonstrated that it is possible to make superconducting finline mixers for frequencies as high as 350 GHz.**

I. Introduction

SUPERCONDUCTOR–INSULATOR–SUPERCONDUCTOR (SIS) MIXERS are the most sensitive coherent detectors of submillimeter radiation. During the past few years, they have been used successfully in submillimeter-wave radio astronomy receivers, giving sensitivities that approach the quantum limit. Recently, there has been considerable interest in developing SIS mixers that are easy to fabricate in large numbers. For example, applications include the 350-GHz focal-plane imaging array HARP, which is currently being developed for the James Clerk Maxwell Telescope in Hawaii, and the large millimeter array (ALMA), which is a major international project to build a 64-element interferometer, covering the frequency range of 100–800 GHz, on a high plateau in Chile. An SIS mixer may be considered suitable for these types of projects if it satisfies the following requirements:

- an antenna beam with low sidelobes and high aperture efficiency;
- low-noise temperature over a wide frequency band;
- reliable, repeatable, and easy to produce;
- compatible with planar-circuit technology.

Conventional waveguide mixers have produced excellent performance, but they often rely heavily on mechanical tuning. The need for complicated machining makes them difficult and expensive to manufacture. In addition, variations in mechanical tolerances, from one mixer to another, often leads to variations in performance. An alternative design, which became popular recently, is the quasi-optical mixer [1]. This design avoids the difficulty of machining mixer blocks by feeding the SIS tunnel junction from a pair of slot antennas, which are placed at the back of a hemispherical lens. Although the quasi-optical mixer has produced impressive noise temperatures, there is some debate as to whether these antennas are as good as horn antennas for closed-packed imaging arrays or applications where the optical coupling is critical.

In this paper, we investigate an alternative possibility and describe the design of a 350-GHz antipodal finline mixer, which satisfies the above requirements [2]. The mixer is fed by a horn–reflector antenna to ensure low sidelobe levels and high beam directivity. The mixer chip itself comprises an antipodal finline, a miniature superconducting microstrip transmission line, and an SIS Nb–AlOx–Nb tunnel junction. In this way, both the RF and IF signals eventually propagate in a microstrip circuit independent of the waveguide modes. In other words, the back of the finline chip, which carries RF power, does not need to be surrounded by waveguide once the incoming power is converted into the microstrip mode. An important advantage is that additional circuitry, such as microstrip image-separating circuits, can be elegantly incorporated once the basic mixer has been designed [3].

A key feature of the arrangement is the use of a low-impedance antipodal finline to transform the waveguide mode into microstrip. The two superconducting films, which form the finline, are deposited on one side of a quartz substrate, and are separated by an oxide layer of just 400-nm thick. Since the thickness of the oxide layer cannot easily be made much greater than 400 nm, and the width of the microstrip line cannot be made much narrower than $\approx 3\ \mu$m, the embedding impedance of the device is low. More precisely, using a microstrip width of $w = 3\ \mu$m, a dielectric thickness of $h = 400$ nm (dielectric constant of $\mathrm{SiO} = 5.8$), and a metallization thickness of $\Delta t = 300$ nm, we obtain a source impedance of 20 Ω [4]. This impedance level is ideal for SIS mixers since it allows a relatively large junction area, which is easier to fabricate. To realize these advantages, the finline taper needs to be designed carefully. The biggest challenge is matching the large impedance of the waveguide to the low impedance of the miniature superconducting microstrip transmission line. In addition, the capacitance of the tunnel junction needs to be matched accurately if the mixer is to achieve the desired center frequency (we no longer have recourse to mechanical tuning).

In this paper, we describe in some detail the design of the various transmission lines and tuning circuits. We compare various ways of calculating finline parameters. This study is critical because of the rather extreme nature of the particular geometry (only 400 nm of oxide) used. We also consider in some

Manuscript received March 1, 1999; revised August 6, 1999.

G. Yassin, S. Withington, and M. Buffey are with the Department of Physics, University of Cambridge, Cambridge CB3 0HE, U.K.

K. Jacobs and S. Wulff are with I. Physikalisches, University of Cologne, Cologne D-50937, Germany.

Publisher Item Identifier S 0018-9480(00)02535-7.

0018–9480/00$10.00 © 2000 IEEE

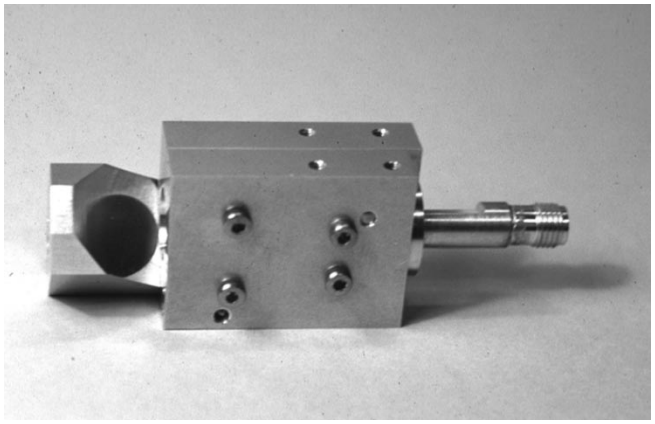

Fig. 1. 350-GHz finline mixer with a horn–reflector antenna.

detail how the analysis methods can be combined into synthesizing (through the "optimum taper method") finline tapers for SIS mixers. Overall, we show that by calculating the electrical parameters accurately, we can obtain a good match between the source and device over a large range of frequencies. Consequently, we can produce a low-noise mixer with a high-quality antenna and no mechanical tuning.

II. Mixer Feed

A. Horn–Reflector Antenna

The horn–reflector antenna is an offset parabolic reflector, which is fed by a smooth-wall or a corrugated metallic waveguide horn (Fig. 1). This arrangement produces a highly collimated beam without the use of plastic lenses. We have already reported that it provides an efficient way of coupling, with low sidelobes and low cross polarization, SIS mixers to a large antenna [5]. An important advantage of this antenna is that it can be machined directly into two halves of a split aluminum block. The resulting antenna is light weight and suitable for imaging arrays.

In a previous publication, we presented a detailed theoretical analysis of the electrical properties of a horn–reflector antenna, fed by a corrugated horn [6]. In this study, we used a smooth-walled conical horn for ease of fabrication and, therefore, we shall simply quote the final results relevant to a smooth-wall feed.

Let E_ρ and E_η be, respectively, the radial and tangential components of the TE_{11} electric field in a circular waveguide of radius a. For longitudinal antenna polarization, the fields can be written as

$$E_\rho = \frac{1}{\kappa\rho} J_1(\kappa\rho)\cos\eta \tag{1}$$

$$E_\eta = -\frac{1}{2}\Big[J_0(\kappa\rho) - J_2(\kappa\rho)\Big]\sin\eta \tag{2}$$

and for transverse polarization by

$$E_\rho = \frac{1}{\kappa\rho} J_1(\kappa\rho)\sin\eta \tag{3}$$

$$E_\eta = \frac{1}{2}\Big[J_0(\kappa\rho) - J_2(\kappa\rho)\Big]\cos\eta \tag{4}$$

where ρ and η are, respectively, the radial and azimuthal coordinates, and κ is the cutoff wavenumber of the dominant mode. The fields in the aperture of the horn can be mapped onto the coordinate system in the projected aperture plane by using a conformal transformation. Once the Cartesian components of the field in the projected aperture are known, the principal radiation patterns of the antenna can be calculated. Although various methods could be used, the Gaussian beam-mode diffraction method is particularly suitable for submillimeter-wave systems. For any polarization, the radiated field can be expanded as a sum of Gaussian–Hermite modes [7]

$$E(x, y, z) = \sum_{mn} A_{mn}\psi_{mn}(x, y, z) \tag{5}$$

with each mode having the form

$$\begin{aligned}\psi_{mn}(x, y, z) = {} & \frac{\sqrt{2}}{w(z)} h_m\left[\frac{\sqrt{2}x}{w(z)}\right] h_n\left[\frac{\sqrt{2}y}{w(z)}\right] \\ & \cdot \exp\left[j(m+n+1)\tan^{-1}\left(\frac{z}{z_c}\right)\right] \\ & \cdot \exp\left[\frac{-j\pi(x^2+y^2)}{\lambda R(z)}\right]\exp[-jkz]\end{aligned} \tag{6}$$

where

$$h_p(u) = \frac{H_p(u)e^{-u^2/2}}{\left(\sqrt{\pi}2^p p!\right)^{1/2}} \tag{7}$$

and $H_p(u)$ is the Hermite polynomial of order p in u; $h_p(u)$ is a set of functions orthonormal over any (x, y) plane. The mode coefficients can be determined by evaluating overlap integrals over the projected aperture plane

$$A_{mn} = \int_{-\infty}^{\infty} E(x, y, 0)\frac{\sqrt{2}}{w_0} h_m\left[\frac{\sqrt{2}x}{w_0}\right] h_n\left[\frac{\sqrt{2}y}{w_0}\right] dx\, dy. \tag{8}$$

Since the phase of the field in the projected aperture plane is flat, the mode coefficients are real. Once the mode coefficients have been determined, it is straightforward to recompose the field at any distance from the projected aperture plane.

III. Mixer Chip

A. General Description

A magnified view of the mixer chip, which shows the finline taper, the RF choke, the tuning stub, and the IF bond pads, is shown in Fig. 2. A dimensioned drawing is shown in Fig. 3 for clarity.

The RF path comprises a transition from waveguide to modified antipodal finline to microstrip. The fins, which form the base and the wiring layers of the tunnel junction, are made out of 300-nm-thick Nb and are separated by 400 nm of SiO. The whole structure is deposited on one side of 90-μm quartz substrate.

Before the fins overlap, the thickness of the SiO is much less than that of the quartz and, hence, the transmission line behaves as a unilateral finline on a quartz substrate. The impedance in this section is several-hundred ohms, which is too high for SIS

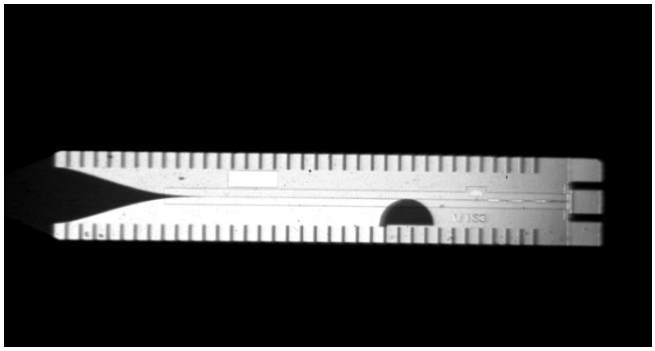

Fig. 2. Magnified photograph of the mixer chip.

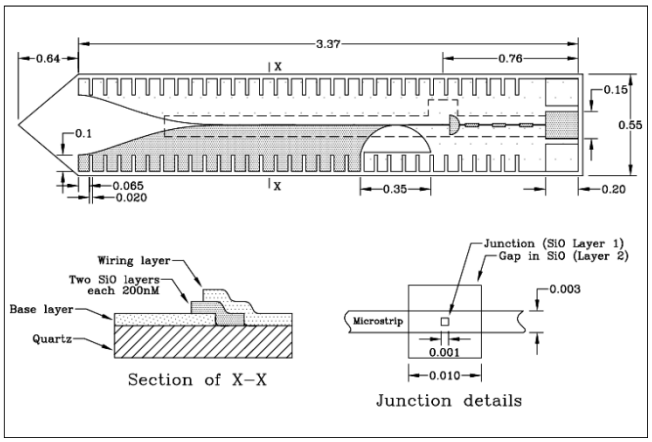

Fig. 3. Drawing of the 350-GHz finline chip with real dimensions (drawing is not to scale).

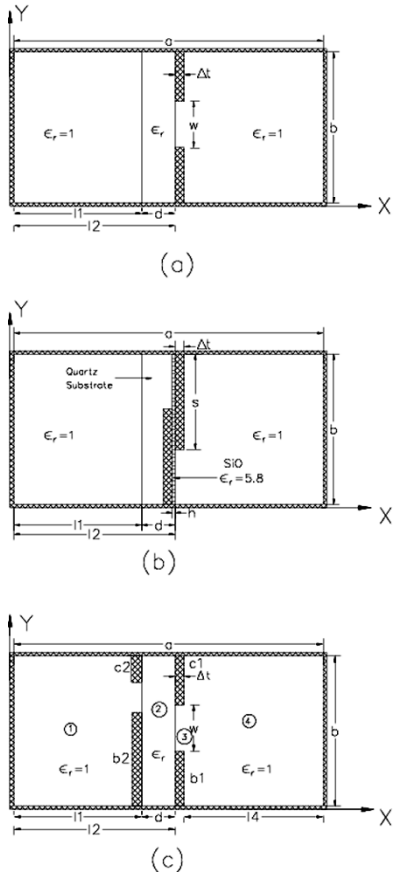

Fig. 4. Arrangements for calculating the electrical parameters of finlines. (a) Unilateral finline for the TR method. (b) Modified antipodal finline for SDA. (c) General finline configuration for the mode-matching method.

tunnel junctions. As the fins overlap, the structure behaves like a parallel-plate waveguide with an effective width equal to that of the overlap region. When the width becomes large enough such that fringing effects can be ignored, a transition to microstrip is performed, which, in turn, is tapered to the required width of 3 μm. The electrical properties of the transmission line are now mainly determined by the thickness of the deposited SiO layer rather than those of the quartz substrate. The quartz substrate is made relatively thick (26% of the waveguide height) to ensure that the structure is robust and easily handled.

B. Calculation of the Finline Parameters

For a variety of reasons, full-wave analysis of the SIS finline taper using a single theoretical method is very difficult. First, the lateral dimensions of the finline vary from being comparable to the waveguide height, through zero, through to a significant overlap. This means that this method needs to account for both dispersion and metallization thickness. To avoid this complication, we designed the waveguide to microstrip transition by dividing the finline taper into three distinct sections. The first section consists of the nonoverlapping fins, which can be considered to be a unilateral finline on a quartz substrate, since the thickness of the SiO layer is much less than that of the quartz substrate. The parameters of this section could be calculated accurately using spectral-domain analysis (SDA), or within an accuracy of $\approx$5% using the much faster transverse resonance (TR) method. We should emphasize that the method of synthesis employed only requires the propagation constant and the cutoff frequencies to be known and does not need the characteristic impedance.

Application of the TR method to find the cutoff frequency of unilateral finlines has been reported for infinitely thin metallization [8]. Assuming a finite metallization thickness Δt, the TR equation for the loaded waveguide (see Fig. 4) can be written

$$-\cot(k_c l_1)-\cot\left[k_c(a-l_2-\Delta t)\right]+\frac{b}{w}\tan(k_c\Delta t)+\frac{B}{Y}=0 \tag{9}$$

where k_c is the cutoff wavenumber and B/Y is the normalized susceptance of the gap. Expressions for the normalized susceptance may be derived using an equivalent circuit for a centered gap unilateral finline, giving the following result:

$$\begin{aligned}
&\frac{B}{Y}=\frac{b}{\pi}k_c[2P_1+\epsilon_r(P_2+P_3)]\\
&P_1=\ln\left[\csc\left(\frac{\pi w}{2b}\right)\right]\\
&P_2=r_d\cdot\arctan\left(\frac{1}{r_d}+\ln\sqrt{1+r_d^2}\right)\\
&P_3=r_b\cdot\arctan\left(\frac{1}{r_b}+\ln\sqrt{1+r_b^2}\right)\\
&r_d=w/d\quad r_b=w/b.
\end{aligned} \tag{10}$$

The propagation constant β is found from the calculated cutoff frequency using the equivalent dielectric constant ϵ_{eq}

$$\beta/k_\circ = \sqrt{\epsilon_{eq}\left[1-\left(\frac{f_c}{f}\right)^2\right]}$$
$$\epsilon_{eq} = (f_{c\circ}/f_c)^2 \tag{11}$$

where $f_\circ$ is the cutoff frequency for $\epsilon_r = 1$.

The second section consists of the overlapping fins and was designed using the SDA method corrected by Wheeler's approximation for the finite thickness of the metallization [9]. Let E_y and E_z represent the tangential electric fields across and along the gap, and let J_y and J_z represent the transverse and longitudinal currents in the fins. The Fourier transform of these quantities are related linearly by the spectral dyadic Greens function as follows:

$$\begin{pmatrix}\tilde{J}_y(\alpha_n)\\ \tilde{J}_z(\alpha_n)\end{pmatrix} = \begin{bmatrix}G_{yy}(\alpha_n,\beta) & G_{yz}(\alpha_n,\beta)\\ G_{zy}(\alpha_n,\beta) & G_{zz}(\alpha_n,\beta)\end{bmatrix}\begin{pmatrix}\tilde{E}_y(\alpha_n)\\ \tilde{E}_z(\alpha_n)\end{pmatrix} \tag{12}$$

where $\alpha_n = n\pi/b$ is the Fourier parameter of the y-coordinate and $G(\alpha,\beta)$ is the dyadic Green's function in the Fourier domain. It has been shown that the dyadic Green's function for the antipodal finline alternates between the Green's function of the two layer (bilateral) and three layer (unilateral) configurations, depending on the parity of n [9]. The above matrix equation is solved as usual [10] using Galerkin's method, which requires expanding the electric fields into a set of basis functions ξ and η

$$\tilde{E}_y(\alpha_n) = \sum_{i=1}^{M} a_i\tilde{\xi}_i(\alpha_n) \tag{13}$$

$$\tilde{E}_z(\alpha_n) = \sum_{i=1}^{M} b_i\tilde{\eta}_i(\alpha_n). \tag{14}$$

We recommend Legendre polynomials for the transverse field and sinusoidal functions for the longitudinal field. This is because Legendre polynomials yield accurate results for both wide and narrow gaps, provided that at least the first five terms are used. It is worthwhile mentioning that we investigated other popular nonorthogonal basis functions, which work well and lead to fast converging solutions for microstrip and unilateral finlines, but gave less accurate results for the antipodal section. Using the geometry of Fig. 4(b), we, therefore, write

$$\xi_m(y) = P_{(m-1)}(u)$$
$$\eta_m(x) = \sin\frac{m\pi}{2}(u+1) \tag{15}$$

where

$$u = \frac{y-(b+s)/2}{(b-s)/2}, \qquad s \le y \le b,\ (-1 \le u \le +1),$$
$$\text{at } x = a/2.$$

We have employed the spectral-domain technique to calculate the cutoff frequency and propagation constant of the overlapping section of fins, neglecting the effect of the quartz substrate. This approximation is good provided the overlap width is larger than the thickness of the 400-nm SiO layer, which separates the fins. We believe that the influence of the errors caused by this approximation is not significant considering the tolerances inherent in the fabrication of the chip, and that the middle section boundaries are slightly modified to smoothly join the rigorously synthesized outer sections.

The third section is a microstrip line, and we have already treated this geometry rigorously, by employing conformal mapping, in a previous paper [4].

C. Mode-Matching Approach

Although the design method described above worked well and produced two good mixers, it was based on splitting the finline taper into two sections. This approach, however, tends to lengthen the taper unnecessarily. A long taper increases the total IF capacitance of the chip and introduces loss at frequencies near the superconducting energy gap. It is desirable, therefore, to develop a single method that is capable of handling the two finline geometries simultaneously, as a single transmission line. Toward this end, we have employed a mode-matching method to calculate the cutoff frequencies of the finline modes for arbitrary metallization thicknesses [11]. The arrangement used is shown in Fig. 4(c).

We first write the expressions for the electromagnetic fields at cutoff in the various regions across the waveguide and then match those fields at the finline discontinuities. In this way, we derived an eigenvalue equation, which allows us to find the cutoff frequencies and expansion coefficients of the finline fields. It can easily be seen that this method does indeed allow us to deal with the three main finline configurations without further difficulties. For example, a gap-centered unilateral finline is obtained by taking $b_1 = c_1 = 0$, $b_2 = c_2$ and an antipodal finline is obtained for $b_1 = c_2 = 0$, $c_1 = b_2$. Derivation of the final eigenvalue equation is laborious; hence, for convenience, we shall only quote the final result. We shall then illustrate the method by calculating the cutoff frequencies of a unilateral finline having a metallization thickness of Δt and compare the results with those obtained by using the spectral-domain and TR methods.

Assume that at cutoff, the hybrid finline mode HE_{mn} becomes a purely TE_{mn}-type mode with cutoff propagation constant $k_{cmn} = k_c$. By equating the transverse components of fields at the interfaces $x = l_1$, $x = l_2$, and $x = l_2 + \Delta t$, we obtain a set of homogeneous equations, which can be expressed by the vector equation [12]

$$\left[\hat{\boldsymbol{H}}(k_c)\right]\vec{\boldsymbol{A}} = \vec{\mathbf{0}} \tag{16}$$

where $\vec{\boldsymbol{A}}$ is an $(n+1)$-element vector, which includes the expansion coefficients $A_0, A_1, A_2, \cdots, A_n$, and $[\hat{\boldsymbol{H}}(k_c)]$ is an $(n+1)\times(n+1)$ matrix with components H_{tp} given by

$$H_{tp} = F_{tp}(w/b)u_p(k_{xp}) - \Delta_t(1+\epsilon_p)\delta_{tp} \tag{17}$$

$$\Delta_t = \left(\frac{\Delta t}{d}\right)\cdot(k_c d) \tag{18}$$

$$\epsilon_p = \begin{cases}1, & p=0\\ 0, & p\neq 0\end{cases} \tag{19}$$

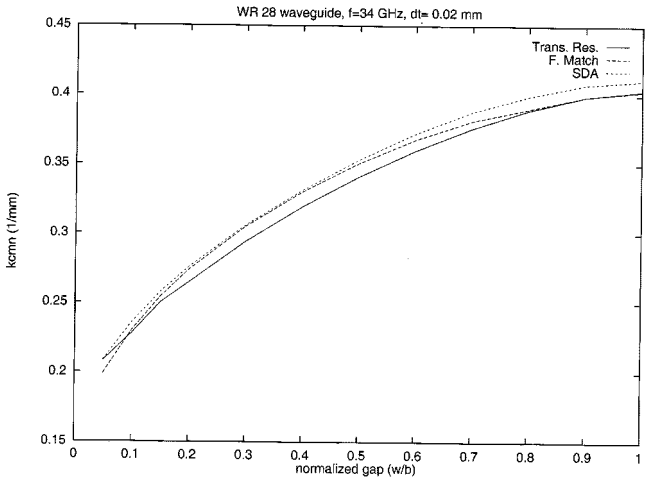

Fig. 5. Comparison of cutoff wavenumber versus normalized gap width in a unilateral finline in WR 28 waveguide ($a = 7.112, b = 3.556, d = 0.25$, and $\epsilon_r = 3.8$).

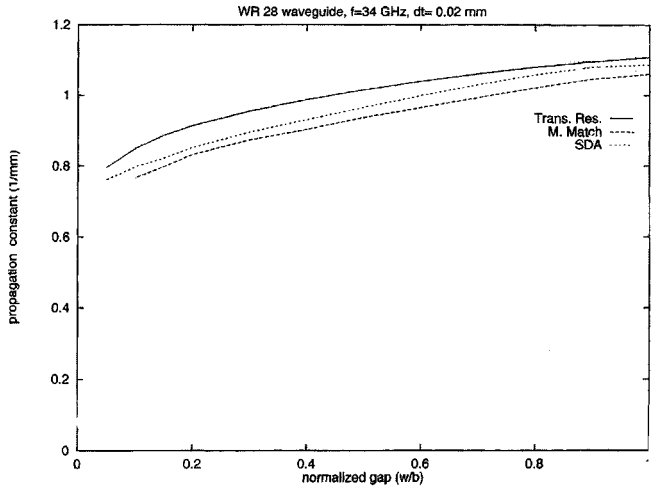

Fig. 6. Comparison of propagation constant versus normalized gap width in an antipodal finline in WR 28 waveguide (dimensions as in Fig. 5).

$$F_{tp} = b/w \sum_{s=0}^{\infty} \frac{1}{(1+\epsilon_s)} P_{ts} P_{ps} \tag{20}$$

$$P_{mn} = 2/b \int_0^w \cos\frac{m\pi}{b}(y+b1)\cos\frac{n\pi}{w} y\, dy. \tag{21}$$

The transverse cutoff propagation constants are given by

$$k_{x01,3,4} = k_c,\ k_{x02} = \sqrt{\epsilon} k_c, \qquad \text{for } p = 0 \tag{22}$$

$$k_{xp}^2 = k_{cmn}^2 - k_{yp}^2, \qquad \text{for } p > 0 \tag{23}$$

$$k_{yi} = \begin{cases} i\pi/b, & \text{in regions 1, 2, 4} \\ i\pi/w, & \text{in region 3.} \end{cases} \tag{24}$$

Assuming, for simplicity, that the dielectric substrate is symmetrically located so that $l_1 = l_4 = l = (a - d - \Delta t)/2$, then the function u_p will have a simple analytical expression as follows:

$$u_p = f_{p1} + h_p f_{p2} \tag{25}$$

where

$$f_{p1} = \frac{\cot k_{xp1} l}{k_{xp1}/k_c} + \epsilon_r \frac{\cot k_{xp3} d}{k_{xp3}/k_c} \tag{26}$$

$$f_{p2} = \frac{\epsilon_r}{\cos k_{xp3} d} \frac{\cot k_{xp3} d}{k_{xp3}/k_c} \tag{27}$$

and $h_p = D_p/A_p$ is the function that relates the coefficients in region 1 to those in region 4. h_p can be written as follows:

$$h_p = -\frac{f_{p2}}{f_{p1} - \Delta_t} \quad \text{for a unilateral finline} \tag{28}$$

$$h_p = (-1)^{p+1} \quad \text{for an antipodal finline.} \tag{29}$$

To investigate the reliability of the mode-matching method, we have calculated the cutoff frequency of a unilateral finline using a WR28 waveguide, and compared the results with those obtained using the TR and SDA methods (see Fig. 5). We assumed a metallization thickness of 0.02 mm, which is small enough to make comparison with (SDA) meaningful, but large enough to make the field-matching solution reliable. When using modal matching, we needed a matrix of about 30 × 30, and it was sufficient to sum over less then 50 terms in order to calculate the matrix elements. A plot of the cutoff propagation constant as a function of normalized gap width is shown in Fig. 6; the same dimensions were used as those in Fig. 5. Clearly, the three methods agree well with each another and, in particular, mode matching agrees very well with the rigorous SDA. Finally, we used the same computed data to calculate the propagation constant as a function of the gap width, using the concept of equivalent dielectric constant introduced above. The agreement between (SDA) and (MM) is excellent for all gap dimensions, as can be seen in Fig. 6.

D. Taper Synthesis

We designed the finline taper using the "optimum taper method" [13], which only requires knowledge of the propagation constant and cutoff frequency as a function of lateral dimensions. This method is based on minimizing the coupling coefficient between the incident and reflected waves, in the z-direction, along a quasi-TEM transmission line. The end product is a minimum-length high-pass section, which gives a return loss lower than a specified design value $R_{\max}$ at frequencies above a predetermined frequency f_0. The reflection coefficient of a TEM taper of length L can be approximated by

$$R(f_\circ, L) = C \int_0^{2\theta} K(\xi) \exp\Big[-j\xi\Big]\, d\xi \tag{30}$$

where $\xi(z) = \int_0^z 2\beta(f_0 z')\, dz'$, $2\theta = \xi(L)$, $K(\xi)$ is the coupling distribution function [13] and C is a normalization constant so that

$$\int_0^{2\theta} K(\xi)\, d\xi = 1 \tag{31}$$

which yields [14]

$$C = \ln\left[\frac{f_{c1}}{f_{c2}}\left(\frac{1 - f_{c2}^2/f_\circ^2}{1 - f_{c1}^2/f_\circ^2}\right)^{1/4}\right]. \tag{32}$$

Here, f_{c1} and f_{c2} are the cutoff frequencies at the two ends of the taper. For a given distribution $K(\xi)$, we can then calculate the required length of taper (or the value of θ), which yields a return loss that is less than the specified design value $R_{\max}$. Moreover, the distribution that gives the minimum value of R for a given length is the Dolph–Chebyshev polynomial [13]. Synthesis of the finline taper then proceeds as follows.

1) Determine the initial and final gaps of the finline section s_1, s_2 and calculate the corresponding cutoff frequencies f_{c1}, f_{c2}.
2) Choose a distribution function $K(\xi)$, which gives the coupling along the taper in the ξ space, which is related to the variable z along the taper by $\xi(z) = \int_0^z 2\beta(f_0, z')\,dz'$. Calculate the normalization constant C and use (30) to determine the value of θ for the specified value of $R_{\max}$.
3) Use the relation between the coupling coefficient and cutoff frequency for both the unilateral and antipodal configurations to obtain the cutoff frequency distribution $f_c(\xi)$. This relation can be written as follows:

$$f_c(\xi) = f_{c1}\left[F/2 + \sqrt{F^2/4 + (1-F)\cdot \exp\left[4CI(\xi)\right]}\right]^{-1/2}$$
$$F = (f_{c1}/f_\circ)^2$$
$$I(\xi) = \int_0^\xi K(\xi')\,d\xi'.$$

4) Calculate the corresponding finline gap from the known cutoff frequency using the TR approach or other method (e.g., SDA) and then synthesize the taper using

$$\Delta z = \frac{\Delta\xi}{2\beta(f_0, \xi)}. \tag{33}$$

The design of the microstrip taper was also based on the above method, but in this case, an analytical expression could be derived to compute the characteristic impedance Z_0 as a function of the longitudinal coordinate z, which can be written [15]

$$Z_0(z) = Z_{01}\exp\left\{\frac{1}{2}\ln\left(\frac{Z_{02}}{Z_{01}}\right)\left[\sin\left[\pi\left(\frac{z}{L} - \frac{1}{2}\right)\right] + 1\right]\right\}. \tag{34}$$

This approach is convenient since the characteristic impedance of a microstrip line is unambiguously defined and can be calculated accurately using the conformal mapping method [4].

We employed the above approach to design the waveguide-to-microstrip transition and found that a taper length of two wavelengths is sufficient to match the 300 Ω impedance of the loaded waveguide to the 15.5 Ω impedance seen by the junction. We verified the integrity of the design method experimentally by performing scale-model measurements at 5 GHz. The measured return loss of a back-to-back finline taper was better than -15 dB over most of the waveguide band.

IV. Device Fabrication

The SIS tunnel junction was fabricated at the University of Cologne, Cologne, Germany, from an Nb–AlOx–Nb trilayer at the same time as the rest of the finline chip. The following four masks were used during fabrication:

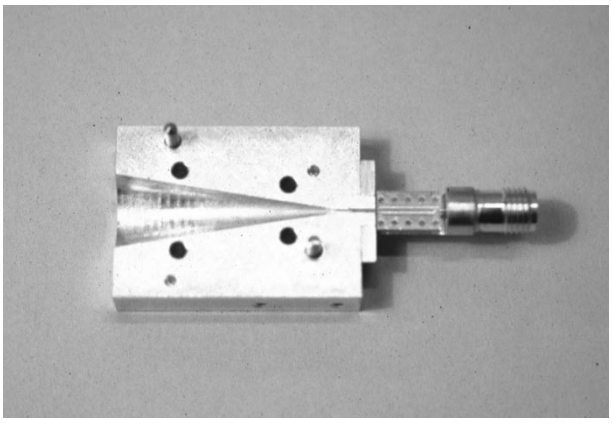

Fig. 7. Lower half of the mixer split block showing the horn, finline chip, and coplanar IF board.

1) base electrode of the finline, which also forms the ground plane of the microstrip;
2) definition of the tunnel junction and a 200-nm layer of SiO;
3) second 200-nm layer of SiO;
4) RF choke, tuning stub, and top finline electrode, which also forms the microstrip line.

The junction used in these experiments had a normal resistance of 25 Ω, a current density of 14 000 A/cm^2, and an area of 0.6 μm^2. The specific capacitance of the junction was 75 fF/μm^2, giving a value of $\omega R_n C \approx 2$. It should be emphasized that the unusually small device area and high current density are not essential features of the finline design. It was noticeable that the device had stronger than usual pair tunneling at zero magnetic field and its I–V characteristic was prone to flux trapping. The high current density of the device may have been a contributing factor. We were nevertheless able to suppress the Josephson tunneling, in the usual way, by the application of a magnetic field parallel to the junction.

V. Mixer Assembly

The chip and IF assembly are shown in Fig. 7. The quartz substrate, which carries the superconducting circuit, is located in the E-plane of a waveguide ($b = 350$ μm, $a = 700$ μm) by machining a groove in the sidewall of a split block. The groove was made 110 μm deep and 110 μm wide in order to accommodate the substrate and serrated choke, respectively. The serrated choke was included in order to cut off high-order modes in the groove. DC bias was supplied to the junction by a bias tee and the magnetic field required to suppress the Josephson effect was supplied by a superconducting coil concentric with the waveguide. We used 2000 turns of 70-μm-diameter Nb wire on a former having a diameter of 7.4 mm. With this arrangement, we swept through several Josephson nulls on increasing the coil current from 0 to 300 mA. The IF output, at 3.5–4.5 GHz, was taken from the mixer chip by bonding 50-μm wires to Palladium pads and connecting them to a ground-backed coplanar transmission line, which led to SMA connectors. The capacitance of the junction was tuned out using an inductive microstrip, terminated by a short-circuit radial stub [16]. The stub could be laid out either as part of the microstrip line (as in Fig. 3) or at right

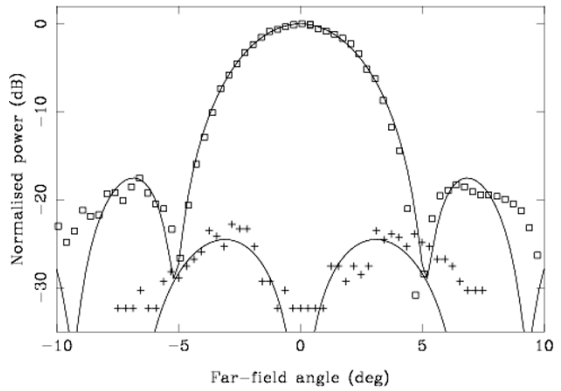

Fig. 8. Far-field copolar and cross-polar radiation patterns in the longitudinal and transverse directions, respectively.

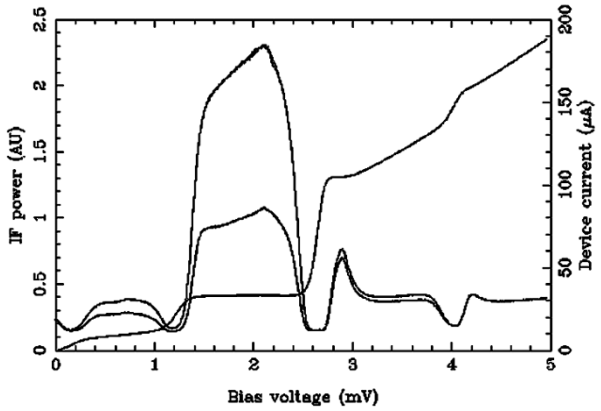

Fig. 9. IF power as a function of bias voltage for hot (300 K) and cold (77 K) loads with a 352-GHz local oscillator. The dc *I-V* curve is also shown.

angle to it. In the former case, the stub could also serve as part of the RF choke circuit.

VI. Experimental Results

First, we measured the radiation patterns of the conical horn–reflector antenna by using the mixer as a direct detector [17]. A varactor-multiplied Gunn oscillator was used in conjunction with a corrugated horn antenna as the source. The Dewar, containing the mixer, was placed on a rotary table, and the projected aperture plane positioned on the axis of rotation. Measurements were made in two linear polarizations. An example is presented in Fig. 8, which shows the copolar radiation pattern in the longitudinal plane [18]. Also included is the cross-polar radiation pattern in the transverse plane. The solid lines represent the theoretical radiation patterns computed using Gaussian–Hermite modes. The copolar radiation patterns show excellent agreement with theory around the main beam, although the poor optical arrangement limited the measurement of the far-out sidelobes. The cross-polar contribution appears to be at about the correct level.

The noise temperature was measured by injecting local-oscillator power into the signal path by means of a partially reflecting Mylar beam splitter. The mixer was cooled to 4.6 K, and a coil current of 88 mA was used to suppress the Josephson effects. Fig. 9 shows the IF response of the mixer at 352 GHz, which gives a noise temperature of 90 ± 3 K. This value was typical for the frequency range of 330–370 GHz, although the performance deteriorated slightly at the edges of the band due to a lack of local-oscillator power.

Although a noise temperature of 90 K is higher than can be achieved at these frequencies, little effort was made to optimize the test arrangement, and more work is required to identify the sources of noise. For instance, optimizing the optical arrangement and IF amplifier should yield lower noise temperatures in the future. Initial assessment suggests that the noise contributions referenced to the input of the receiver are 56 K due to RF coupling losses, 16 K due to the IF amplifier, and 18 K due to the mixer[19].

VII. Conclusion

We have designed and tested an antipodal horn–reflector finline mixer at 350 GHz. We measured the radiation patterns of the horn–reflector antenna and showed that they agree well with theory. Although the cross-polar components were better than -18 dB, our intention is to corrugate the conical horn, as in previous work, and, hence, reduce the sidelobe and cross-polar levels further. We measured a receiver noise temperature of 90 K across the whole of the 330–370-GHz frequency range, and we fully expect to be able to reduce the noise temperature in future tests.

Our study has shown that it is possible to produce fixed-tuned finline SIS mixers for frequencies as high as 350 GHz. These mixers have no mechanical tuning and are easy to fabricate. Ease of fabrication is important when a large number of mixers have to be produced, e.g., for focal-plane imaging arrays or multielement interferometers. A key feature of our design is that the finline geometry allows complicated circuits requiring large areas of the substrate to be produced. We are currently considering the possibility of manufacturing an image-reject mixer, where the signal enters through one end of a piece of waveguide and the local oscillator through the other.

References

[1] J. Zmuidzinas and H. G. LeDuc, "Quasi-optical slot antenna SIS mixer," *IEEE Trans. Microwave Theory Tech.*, vol. 40, pp. 1797–1804, Sept. 1992.

[2] G. Yassin, R. Padman, S. Withington, K. Jacobs, and S. Wulff, "A broad band 230 GHz finline mixer for astronomical imaging arrays," *Electron. Lett.*, vol. 33, pp. 498–500, 1997.

[3] A. R. Kerr and S.-K. Pan, "Design of planar image separating and balanced SIS mixers," in *Proc. 7th Int. Symp. Space Terahertz Technol.*, Charlottesville, VA, Mar. 1996, pp. 207–219.

[4] G. Yassin and S. Withington, "Electromagnetic models for superconducting millimeter-wave and submillimeter-wave microstrip transmission line," *J. Phys. D, Appl. Phys.*, vol. 28, pp. 1983–1991, 1995.

[5] S. Withington, G. Yassin, M. Buffey, and C. Norden, "A horn–reflector antenna for high performance submillimeter imaging arrays," *Int. J. Infrared MIllim. Waves*, vol. 18, no. 2, pp. 341–358, 1997.

[6] G. Yassin, M. Robson, and P. J. Duffett-Smith, "The electrical characteristics of a conical horn–reflector antenna employing a corrugated horn," *IEEE Trans. Antennas Propagat.*, vol. 41, pp. 357–361, Apr. 1993.

[7] S. Withington and J. A. Murphy, "Multimode Gaussian optics," in *Proc. 3rd Int. THz Electron. Workshop*, Zermatt, Switzerland, Aug./Sept. 1995.

[8] C. Schieblich, J. K. Piotrowski, and J. H. Hinken, "Synthesis of optimum finline tapers using dispersion formulas for arbitrary slot width and locations," *IEEE Trans. Microwave Theory Tech.*, vol. MTT-30, pp. 1638–1644, Dec. 1984.

[9] D. Mirshekar-Syahkal and J. B. Davies, "An accurate, unified solution to various finline structures, of phase constant, characteristic impedance and attenuation," *IEEE Trans. Microwave Theory Tech.*, vol. MTT-30, pp. 1854–1861, Nov. 1982.
[10] L. P. Schmit and T. Itoh, "Spectral domain analysis of dominant and higher order modes in finlines," *IEEE Trans. Microwave Theory Tech.*, vol. MTT-28, pp. 981–985, Sept. 1980.
[11] A. M. K. Saad and K. Schunemann, "Closed form approximations for finline eigenmodes," *Proc. Inst. Elect. Eng.*, pt. H, vol. 129, no. 5, pp. 253–261, 1982.
[12] G. Yassin, S. Withington, K. Jacobs, and S. Wulff, "Design of a broad band finline mixer for 350–450 GHz," in *Proc. 5th Int. THz Electron. Workshop*, Grenoble, France, Sept. 1997, pp. 19–27.
[13] F. Sporleder and H. G. Unger, *Waveguide Tapers Transitions and Couplers*. Stevenage, U.K.: Peregrinus, 1979.
[14] J. H. Hinken, "Simplified analysis and synthesis of finline tapers," *Arch. Elektr. Uebertrag. Tech.*, vol. 37, pp. 375–380, 1983.
[15] D. P. McGinnis and J. B. Beyer, "A broad-band microwave superconducting thin-film transformer," *IEEE Trans. Microwave Theory Tech.*, vol. 36, pp. 1521–1525, Nov. 1988.
[16] B. A. Syrett, "A broad band element for microstrip bias or tuning circuits," *IEEE Trans. Microwave Theory Tech.*, vol. MTT-28, pp. 925–927, Aug. 1980.
[17] S. Withington, K. G. Isaak, S. A. Kovtonyuk, R. A. Panhuyzen, and T. M. Klapwijk, "Direct detection at submillimeter wavelengths using superconducting tunnel junctions," *Infrared Phys. Technol.*, vol. 36, pp. 1059–1075, 1995.
[18] A. B. Crawford, D. C. Hogg, and L. E. Hunt, "A horn–reflector antenna for space communication," *Bell Syst. Tech. J.*, vol. 40, pp. 1095–1116, 1961.
[19] R. Blundell, R. E. Miller, and K. Gundlach, "Understanding noise in SIS receivers," *Int. J. Infrared Millim. Waves*, vol. 13, no. 1, pp. 3–14, 1992.

Ghassan Yassin received the B.Sc. degree in mathematics and the M.Sc. degree in applied physics from Hebrew University, Jerusalem, in 1973 and 1997, respectively, and the Ph.D. degree in physics from Keele University, Staffordshire, U.K., in 1981.

He is currently a Senior Research Associate in the Astrophysics Group, Cavendish Laboratory, University of Cambridge, Cambridge, U.K. His main research interest is in the areas of superconducting submillimeter-wave detectors and terahertz optics.

Stafford Withington (M'89) is currently an Assistant Director of Research in the Astrophysics Group, Cavendish Laboratory, University of Cambridge, Cambridge, U.K. His main areas of interest are in the submillimeter-wave band, where he is involved with optics, detectors, and low-noise instrumentation for astronomy.

Dr. Withington is a Fellow of Downing College, Cambridge, U.K.

Matthew Buffey was born in Stourbridge, U.K., in 1974. He received the physics degree from Leeds University, Leeds, U.K., in 199 , and is currently working toward the Ph.D. degree at Cambridge University, Cambridge, U.K.

He is currently with the Vega Group PLC, under contract from the ESA/ESRIN to develop operational software for processing data from space-borne sensors.

K. Jacobs (M'86) received the Ph.D. degree in physics from the University of Cologne, Cologne, Germany, in 1984.

From 1984 to 1988, he was engaged in the instrumentation of the 3-m radio telescope of the Koelner Observatorium für Submillimeter-Astronomie (KOSMA), Gornergrat near Zermatt, Switzerland. In 1989, he was a Visiting Scientist with the Jet Propulsion Laboratory, Pasadena, CA, where he was involved with a 620-GHz superconducting mixer. After returning to the University of Cologne, he established a laboratory for the development and fabrication of superconducting mixers and currently heads the Superconducting Devices and Mixers Group. Mixers developed by the group are in operation at astronomical observatories including AST/RO, South Pole. His current activities include the development of superconducting mixers for SOFIA and FIRST and several atmospheric physics experiments. He is an Instrument Co-Investigator on the European Space Agency's FIRST mission.

S. Wulff was born in Hamburg, Germany, in 1962. He received the Ingenieur der Physikalischen Technik (physics engineer) degree from the Fachhochschule Luebeck, Luebeck, Germany, in 1990.

Since 1990, he has been with the Superconducting Mixers and Devices Group, KOSMA, University of Cologne, Cologne, Germany, where he is involved in the fabrication of superconducting mixer devices.